

# The Application of Affine/Interval Algebra to Determine the Time of Concrete Cover Damage in Reinforced Concrete Due to Corrosion

Tomasz KRYKOWSKI

*Silesian University of Technology*  
*Faculty of Civil Engineering*  
*Department of Mechanics and Bridges*  
44-100 Gliwice, Poland  
e-mail: tomasz.krykowski@polsl.pl

This paper presents the application of affine numbers to determine the time of concrete cover cracking in reinforced concrete elements from the initiation of the reinforcement corrosion. This issue is crucial for evaluating sustainability and durability of reinforced concrete structures. The proposed general approach has been used to forecast displacements and crack propagation versus time in reinforced concrete elements subjected to corrosion tests. The affine approach equations describing changes caused by the formation of corrosion products are defined and the corresponding tensor of the volumetric strain rate is formulated. The time of cover cracking has been analysed using the Finite Element Method (FEM) and the Monte Carlo (MC) method to verify the correctness of calculations.

**Keywords:** corrosion, FEM, elastic-plastic, cover cracking, affine numbers.

## 1. INTRODUCTION

Chloride ions and carbon dioxide present in the environment and the effects of direct current leaks from electric tractions cause the corrosion of rebars in concrete and degradation of reinforced concrete structures [31]. These issues are crucial for evaluating sustainable development and the durability of reinforced concrete structures. Greater thickness of reinforced concrete cover has a positive impact on the initiation time of reinforcement corrosion. But, on the other hand, it causes a series of negative effects on the environment, such as increased emission of carbon dioxide [7].

The analysis of the life cycle of structures exposed to corrosion shows it can be divided into four characteristic phases [33]: initiation of reinforcement corrosion

(*in*) (transport of aggressive substances), propagation (*p*) (activation – filling voids in the increased porosity interface transition zone (ITZ) in a concrete structure in the absence or increase of mechanical impacts and local degradation of contact region), cover cracking (*crack*) (caused by an increment of products of reinforcement corrosion) and the accelerated degradation of the structure (*ad*), [6, 32, 33]. Indices (*0*) and (*cr*) are related respectively to activation time and critical time, Fig. 1.

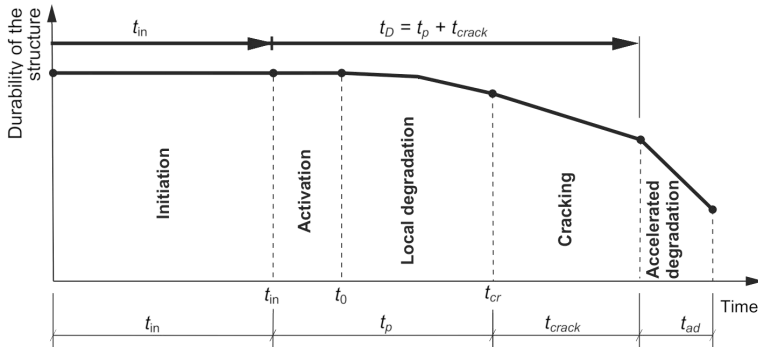


FIG. 1. The evolution of durability of structures over their lifetime.

When considering the durability of a structure, it is crucial to determine the time of degradation  $t_D$  after which the acceptable width of cracks is achieved. In this case, the degradation time is regarded as the sum of the propagation time  $t_p$  and the cracking time  $t_{crack}$ . Among other aspects considered in the paper, the effect of reinforcement corrosion on the degradation time of the cover is discussed with respect to the hierarchical design of structures, whose impact on the environment and total life cycle costs are considered [33]. This approach is important, taking into account the building information modelling (BIM) technologies used to design structures. It also forces the formation of mathematical models to forecast the behaviour of a structure during its life cycle.

This paper focuses on the second and third stages (propagation and cover cracking) of the life cycle. The first stage (initiation of corrosion) refers to the transport of mass, aggressive substances, moisture, and heat into concrete. The scientific literature, inter alia [15, 22, 23, 28, 30], describes in detail this stage.

The stages of propagation and cracking refer to the process of destruction of the concrete structure from the moment of activating the corrosive cells on the reinforcement surface. As a result of the initiated electrode process [1, 9, 10], voids in the transition zone [4] and adjacent concrete are filled with corrosion products. Pressure also increases due to the impact of corrosion products on the concrete. Consequently, the concrete cover is cracked. Many models demonstrat-

ing concrete cracking due to corrosion are described in the scientific literature. They include both the analytical approach [16, 25, 35] and the complex approach, in which FEM is applied [14, 24]. Uncertainty of parameters defining the corrosion process is the main difficulty related to the analysis of corrosion degradation due to reinforcement corrosion in concrete at the propagation stage. The application of methods based on the probabilistic approach [2, 26] is complex due to problems with determining the function of the density of probability parameters defining corrosion.

The approach based on interval analysis is an alternative mathematical description of corrosion problems subject to uncertainty, which usually does not contain probabilistic elements [21]. This method is burdened with an error related to the overestimation of results. Affine numbers in calculations is another approach close to the interval analysis, but without overestimation issues [29].

This paper presents the use of affine numbers to determine the time of concrete cover damage in reinforced concrete elements from the moment of initiating reinforcement corrosion (formation of a corrosion cell). The proposed approach is used to forecast displacement fields and cracks and the propagation of the crack width in a reinforced concrete element subjected to corrosion resulting from the impact of the environment. The interval analysis with the affine approach and INTLAB libraries [27] are used to define equations describing changes caused by the formation of corrosion products, and to formulate the corresponding tensor of the volumetric strain rate. The time of cover cracking is analysed with FEM for upper sup ( $\bar{\varepsilon}^V$ ) and lower inf ( $\underline{\varepsilon}^V$ ) bounds of increments of the tensor of corrosion volumetric strain, which was of affine type. The Monte Carlo (MC) method is used to verify the correctness of calculations [19].

## 2. BASIC ALGEBRAIC OPERATIONS ON AFFINE AND INTERVAL NUMBERS

The main problem concerning the cover durability is the uncertainty of parameters describing the discussed physical and chemical process. Uncertainties are related to, inter alia, the chemical composition of corrosion products, the microstructure of the interface transition zone (transition layer with the increased porosity, the so-called ITZ [4]) and electric current in the electrochemical cell. It is very difficult to determine the probability density function for the majority of parameters used to forecast the durability of reinforced concrete elements. Therefore, affine number  $\bar{X}^A$  was suggested for the description of problems concerning the durability of reinforced concrete elements subjected to corrosion of the reinforcement

$$\bar{X}^A = X_0 + X_1\bar{\varepsilon}_1 + \dots + X_n\bar{\varepsilon}_n, \quad (1)$$

where  $\bar{\varepsilon}_i$  is the noise symbol, whose values are changing within the  $[-1, 1]$  interval,  $X_0$  is the central value, and values of  $X_i$  ( $i > 0$ ) are respectively called partial deviations from that value [5, 11–13, 27]. Arbitrary affine number  $\bar{X}^A$  can be written as an interval number  $\bar{X}^I = [x^-, x^+]$ ,  $x^- < x^+$ ,  $x^- = \inf(\bar{X}^I)$ ,  $x^+ = \sup(\bar{X}^I)$  using the relationships [5, 11]

$$\bar{X}^A = X_0 + \sum_{i=1}^n X_i \bar{\varepsilon}_i \equiv [X_0 - \Delta X, X_0 + \Delta X], \quad \Delta X = \sum_{i=1}^n |X_i|, \quad (2)$$

where  $\Delta X$  is the total number of deviations of affine expression. The inverse approach results in averaging deviations  $X_i$  from the affine number.

Arbitrary interval number  $\bar{X}^I = [x^-, x^+]$  [8] can be converted into affine number  $\bar{X}^A$  using the following relationship [5, 11]:

$$\bar{X}^A = X_0 + X_m \varepsilon_m, \quad X_0 = 0.5(x^+ + x^-), \quad X_m = 0.5(x^+ - x^-), \quad (3)$$

where  $m$  is the noise symbol (in Eq. (3) we do not sum over  $m$ ).

Basic operations on interval numbers present the following relationships [21]:

$$\bar{X}^I \pm \bar{Y}^I = [x^- \pm y^-, x^+ \pm y^+], \quad (4)$$

$$\begin{aligned} \bar{X}^I \cdot \bar{Y}^I = [\min(x^- y^-, x^- y^+, x^+ y^-, x^+ y^+, \\ \max(x^- y^-, x^- y^+, x^+ y^-, x^+ y^+)], \end{aligned} \quad (5)$$

$$\bar{X}^I / \bar{Y}^I = [x^-, x^+] \cdot [1/y^+, 1/y^-]. \quad (6)$$

Basic operation on affine numbers were described, inter alia, in the papers [5, 11–13, 27, 29]:

$$\bar{X}^A \pm \bar{Y}^A = X_0 \pm Y_0 + \sum_{i=1}^n (X_i \pm Y_i) \bar{\varepsilon}_i, \quad (7)$$

$$\bar{X}^A \cdot \bar{Y}^A = X_0 \cdot Y_0 + \sum_{i=1}^n (X_0 Y_i + X_i Y_0) \bar{\varepsilon}_i + \sum_{i=1}^n X_i \bar{\varepsilon}_i \cdot \sum_{i=1}^n Y_i \bar{\varepsilon}_i, \quad (8)$$

$$\bar{X}^A / \bar{Y}^A = \bar{X}^A \cdot (\bar{Y}^A)^{-1} \cong \bar{X}^A \bar{Z}^A. \quad (9)$$

The function  $\bar{Z}^A = 1/\bar{Y}^A$  in Eq. (9) can be determined as described in papers [18, 27] using the Chebyshev approximation. Using INTLAB libraries for calculations, the result of the multiplication is regarded as the common part of actions performed in accordance with (5) and (8), by which the result can never be worse than ordinary interval arithmetic [27].

### 3. IMPACT OF CORROSION PRODUCTS ON COVER CONCRETE USING AFFINE AND INTERVAL APPROACH

The mechanical impact of corrosion products on concrete cover cannot be considered as the initiation of reinforcement corrosion. At the initial stage of corrosion, when the activation time  $t_0$  was achieved and voids in the ITZ were filled [4], the expansion of corrosion products into micro-cracks that propagate in the transition zone between steel and concrete can be observed (the so-called CAR – corrosion accommodation region) and their transport into deeper regions of concrete cover can take place [20]. The kinetics of such changes related to the impact of some corrosion products on concrete could be expressed with the equation describing the rate of change of effective volume of corrosion products  $\dot{V}_{eff}$ , which includes those corrosion products that have a mechanical impact on the concrete cover [34]

$$\begin{aligned} \dot{V}_{eff} &= \dot{V}_{ekw} - \dot{V}_{por} - \dot{V}_{tran}, & \dot{V}_{ekw} &= \dot{V}_R - \dot{V}_{Fe^{2+}}, \\ V_{Fe^{2+}} &= \frac{m_{Fe^{2+}}}{\rho_{Fe^{2+}}}, & \dot{m}_{Fe^{2+}} &= kI = kA_s i. \end{aligned} \tag{10}$$

In Eq. (10),  $\dot{V}_{por}$  is the rate of change in volume of the corrosion products brought into newly created empty spaces and micro-cracks formed in the ITZ at the interface of a rebar and the concrete cover,  $\dot{V}_{tran}$  is the rate of change in volume of corrosion products penetrating into deeper layers of concrete, cf. Fig. 2,  $\dot{V}_{Fe^{2+}}$  is the rate of change in volume of corrosion loss,  $\dot{m}_{Fe^{2+}}$  is the rate of change in the mass of iron ions (Faraday’s law),  $m_{Fe^{2+}}$  is the mass of iron ions,  $\rho_{Fe^{2+}}$  is the density of iron ions,  $k$  is the electrochemical equivalent of iron,  $A_s$  is the corroded area of a rebar,  $i$  is the density of the corrosion current and  $I$  is current intensity. The changes occurring in the cover can be schematically shown in the way presented in Fig. 2 where: 1) cover of concrete, 2) empty pore

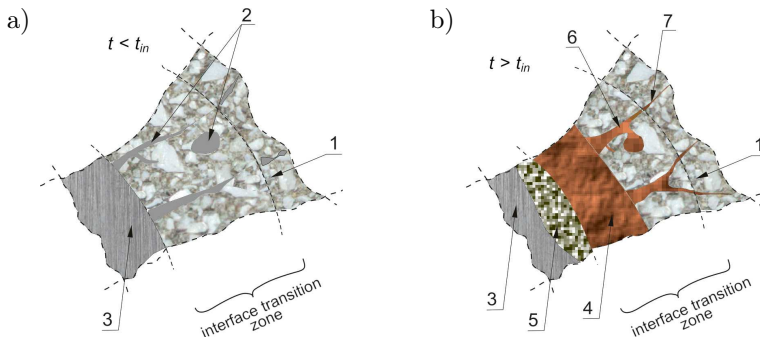


FIG. 2. Kinetics of the reinforcement corrosion processes in the concrete cover: a) inactive corrosion process, b) active corrosion process of the reinforcement (description in the text).

spaces, 3) reinforcing steel, 4) corrosion products, 5) corrosion cavity filled with the volume of corrosion products changing with the velocity  $\dot{V}_{\text{Fe}^{2+}}$ , 6) microcrack volumes filled with corrosion products in the ITZ layer changing with the rate  $\dot{V}_{\text{por}}$ , 7) volume of corrosion products transferred through the pores into the deeper layers of concrete with the rate  $\dot{V}_{\text{tran}}$ .

It is difficult to unambiguously determine  $\dot{V}_{\text{por}}$  and  $\dot{V}_{\text{tran}}$ . However, they can be defined as functions of the formation rate of equivalent volume  $\dot{V}_{\text{ekw}}$  and an additional variable  $\beta$  which specifies the intensity of the impact of the corrosion process on the cover structure [34]

$$\dot{V}_{\text{eff}} = (1 - \beta)\dot{V}_{\text{ekw}}, \quad \dot{V}_{\text{ekw}} = \psi I, \quad \beta\dot{V}_{\text{ekw}} = \dot{V}_{\text{por}} + \dot{V}_{\text{tran}}, \quad (11)$$

$$\psi = \frac{(\alpha^{-1}\vartheta - 1)k}{\varrho_{\text{Fe}^{2+}}}, \quad \alpha = m_{\text{Fe}^{2+}}m_R^{-1}, \quad \vartheta = \varrho_{\text{Fe}^{2+}}\varrho_R^{-1}, \quad (12)$$

where  $\varrho_R$  is the density of corrosion products,  $m_R$  is the mass of corrosion products, and  $\alpha$  and  $\vartheta$  are the adopted parameters depending on the chemical composition of corrosion products [25].

In fact, parameters describing the process of developing a damage in the cover are not of a deterministic type. Parameters describing the chemical composition of corrosion products  $\bar{\alpha}$ ,  $\bar{\vartheta}$  [25], porosity  $\bar{\gamma}_{\text{wp}}$ , the width of the transition zone  $\bar{w}_{\text{wp}}$  and the electrochemical equivalent of iron  $\bar{k}$  are assumed to be uncertain (interval) parameters. As a consequence of the above assumption also physical quantities regarded as deterministic parameters of the volume of porous space  $\bar{V}_{\text{por}}$  and the volume of the transition zone  $\bar{V}_{\text{wp}}$  [4] changed their nature:

$$\bar{V}_{\text{por}} = \bar{\varepsilon}_{\text{wp}}\bar{V}_{\text{wp}} \Rightarrow \bar{V}_{\text{por}} = [V_{\text{por}}^-, V_{\text{por}}^+], \quad (13)$$

$$\bar{V}_{\text{wp}} = \bar{w}_{\text{wp}}\pi D \Rightarrow \bar{V}_{\text{wp}} = [V_{\text{wp}}^-, V_{\text{wp}}^+], \quad (14)$$

where  $D$  is the diameter of the rebar. Taking into account the relationship (11) it is possible to develop an equation based on the concept of affine numbers to describe a change in the effective volume of corrosion products using the interval/affine approach

$$\dot{\bar{V}}_{\text{eff}} = (1 - \beta)\bar{w}\dot{\bar{V}}_{\text{ekw}}, \quad (15)$$

where the parameter  $\bar{w}$  in Eq. (15) includes the effect of uncertainty on the initiation time and the method of the mechanical impact of corrosion products on concrete.

The beginning of the impact of corrosion products on the concrete cover can be observed after the time  $t_0^-$  when voids  $V_{\text{por}}^-$  are filled with the equivalent

volume of corrosion products  $V_{ekw}^+$ . The considered interval numbers provide three possible situations: no interaction  $t < t_0^-$ ,  $V_{ekw}^+ < V_{por}^-$ ,  $\bar{\omega} = [0, 0]$ , the unconditional interaction between corrosion products and the cover are observed  $t > t_0^+$ ,  $V_{por}^+ < V_{ekw}^-$ ,  $\bar{\omega} = [1, 1]$ , and an intermediate situation different from the above situations, in which both cases are possible, is  $t_0^- \leq t \leq t_0^+$ ,  $\bar{\omega} = [0, 1]$ , Fig. 3a. The relationship describing the parameter  $\bar{\omega}$  can be summarised with the following equation:

$$\bar{\omega} = \begin{cases} [0, 0], & t < t_0^-, & V_{ekw}^+ < V_{por}^-, \\ [0, 1], & t_0^- \leq t \leq t_0^+, & V_{por}^- \leq V_{ekw}^+ \wedge V_{ekw}^- \leq V_{por}^+, \\ [1, 1], & t > t_0^+, & V_{por}^+ < V_{ekw}^-. \end{cases} \quad (16)$$

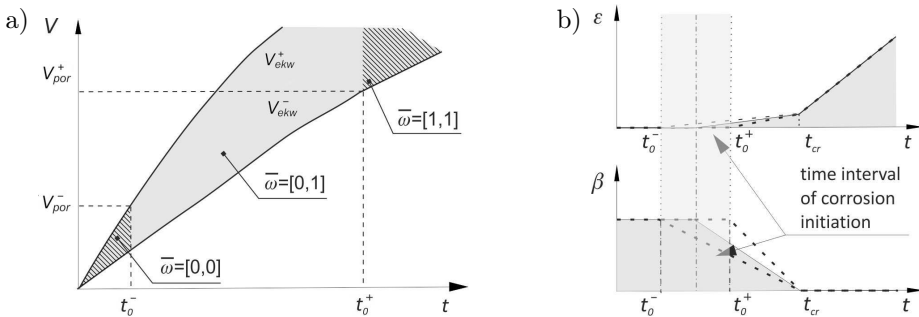


FIG. 3. Evolution of  $\bar{\omega}$  and  $\beta$  parameters over the function of the formation time of corrosion products: a) the range of variability of the interval parameter  $\bar{\omega}$  depending on limit values  $V_{por}^-$ ,  $V_{por}^+$ ,  $V_{ekw}^-$  and  $V_{ekw}^+$ ; b) the range of variability of the function  $\beta$  describing changes in the intensity of the impact of corrosion products on cover concrete.

For the purpose of simplifying the discussion, the function  $\beta$  in (15) was assumed to be deterministic. This function reflects the three phases of interaction between corrosion products and the concrete cover, Fig. 3b. The first phase occurred for  $t \leq t_0^-$  where  $t_0^-$  was the lower bound of the interval determining the activation time  $\bar{t}_0 = [t_0^- t_0^+]$  of the mechanical impact of corrosion products on the concrete cover  $\beta = 1$ , no interaction with the concrete cover. The activation time was identified with the time required for filling voids  $V_{ekw}^+ = V_{ekw}^+(t_0^-) = V_{por}^-$  ( $V_{ekw}^- = V_{ekw}^-(t_0^+) = V_{por}^+$ ). Because of the activation time, understood as the interval variable, it makes the process of determining the parameter  $\beta$  more complicated, and the assumption was made in the present paper that  $t_0^- \approx t_0^+ \approx t_0$ ,  $\Delta t_0 = t_0^+ - t_0^- \ll \Delta t_{cr} = t_{cr} - t_0$ , where  $t_{cr}$  is the critical time specifying the condition under which the whole volume of corrosion products exerted an impact on the cover of concrete  $\beta = 0$ , Fig. 3b. Another impact phase of corrosion products on the concrete cover is the interval  $t_0^- = t_0 \leq t \leq t_{cr}$ , between the activation time  $t_0$  and critical time  $t_{cr}$ ,  $\beta \in (0, 1)$ . During this phase, there

can be observed a gradual increase in the impact of spreading corrosion on the concrete cover. Micro-cracks propagated around the rebar and pores become connected as a result of the formation of micro-cracks. The critical time can be experimentally determined and in some papers identified with the critical volume of corrosion products  $V_{cr}$  or  $V_{car}$  (corrosion accommodation region) [20]. However, using the term  $V_{car}$  is not precise and this value is difficult to determine experimentally. The final, third stage took place for  $t > t_{cr}$  ( $\beta = 0$ ), and the formation of resulting corrosion products had a significant impact on concrete cover  $\dot{V}_{eff} = \dot{V}_{ekw}$ . The  $\beta$  function can be described by the relationship [20, 34]

$$\beta = \begin{cases} 1, & t < t_0 \approx t_0^-, & V_{ekw}^+ < V_{por}^-, \\ (t_{cr} - t)/(t_{cr} - t_0), & t_0 \approx t_0^- \leq t \leq t_{cr}, & V_{por}^- \leq V_{ekw}^+ \wedge V_{ekw}^- \leq V_{cr}, \\ 0, & t > t_{cr}, & V_{ekw}^- > V_{cr}. \end{cases} \quad (17)$$

In the case of deterministic description, the volumetric strain in the cover resulting from the corrosion propagation could be defined by analysis of the rate of change of the first invariant of volumetric strain tensor  $\dot{I}_{\varepsilon^V}$ ,

$$\dot{I}_{\varepsilon^V} \approx \frac{\dot{V}_{eff}}{V_0} = \dot{\varepsilon}_{11}^V + \dot{\varepsilon}_{22}^V + \dot{\varepsilon}_{33}^V, \quad (18)$$

where  $V_0$  is the initial volume; however,  $\dot{\varepsilon}_{kk}^V$  is a component of the rate of volumetric strain tensor caused by products of corrosion, and  $k$  is the index ( $k = 3$  relates to the direction parallel to the rebar's axis).

In the analysis of the reinforcement corrosion process, in the deterministic variant we can consider three situations [36]. The first is for  $t \leq t_0$ . The increase in volumetric strains caused by corrosion products in the time range of the corrosion process is isotropic  $\dot{\varepsilon}_{11}^V = \dot{\varepsilon}_{22}^V = \dot{\varepsilon}_{33}^V = \dot{\varepsilon}^V$ . Another intermediate case takes place for  $t_0 \leq t \leq t_{cr}$ , where we can see compacting of the corrosion products in the ITZ layer,  $\dot{\varepsilon}_{11}^V = \dot{\varepsilon}_{22}^V = \dot{\varepsilon}^V$ ; however, the value  $\dot{\varepsilon}_{33}^V \in (0, \dot{\varepsilon}^V)$ . The last situation is for  $t > t_{cr}$ . We assume that in this period of time the layer of corrosion products is compacted, which prevents the formation of corrosion deformations along the axis of the reinforcing bar  $\dot{\varepsilon}_{33}^V = 0$ ,  $\dot{\varepsilon}_{11}^V = \dot{\varepsilon}_{22}^V = \dot{\varepsilon}^V$ . Increments in the volume of corrosion products could only be observed in the plane perpendicular to the rebar axis. In the affine/interval description, the above-mentioned consideration can be shown in the form of the equations:

- The initial stage,  $t \leq t_{cr}$

$$\dot{\varepsilon}_{\alpha\beta}^V = \frac{\lambda(1 - \beta)\bar{\omega}(\bar{\alpha}^{-1}\bar{\vartheta} - 1)\bar{k}}{\eta \varrho_{Fe^{2+}} + V_0} \bar{I} \delta_{\alpha\beta}, \quad (19)$$

$$\bar{I} = A_s \bar{I}, \quad \dot{\varepsilon}_{33}^V = \beta \dot{\varepsilon}_{\alpha\beta}^V, \quad \alpha, \beta = 1, 2,$$

$$\eta = 3\beta + 2(1 - \beta); \tag{20}$$

- Active corrosive damage of the cover, for  $t > t_{cr}$

$$\dot{\varepsilon}_{\alpha\beta}^V = \frac{\lambda\bar{\omega} (\bar{\alpha}^{-1}\bar{\vartheta} - 1) \bar{k}}{2 \varrho_{Fe^{2+}} V_0} \bar{T} \delta_{\alpha\beta}, \quad \dot{\varepsilon}_{33}^V = 0, \quad \bar{T} = A_s \bar{i}. \tag{21}$$

The parameter  $\eta$  used in Eqs (20)–(22) takes into account the effect of the expansion of corrosion products in the transition zone. The parameter  $\lambda$ , which can generally be regarded as the interval parameter, can represent the situation observed, inter alia, during tests on accelerated corrosion when some corrosion products are washed out into the solution without producing any mechanical effects.

#### 4. APPLICATION OF AFFINE NUMBERS TO EVALUATE THE DURABILITY OF REINFORCED CONCRETE SUBJECTED TO CORROSION

The reinforced concrete element with dimensions of  $800 \times 100 \times 160$  mm, reinforced with the steel rebar  $\phi 20$ , was subjected to numerical analysis. The analysis included an isolated part of the structure with the length of 80 mm, which with the MES mesh is illustrated in Fig. 4.

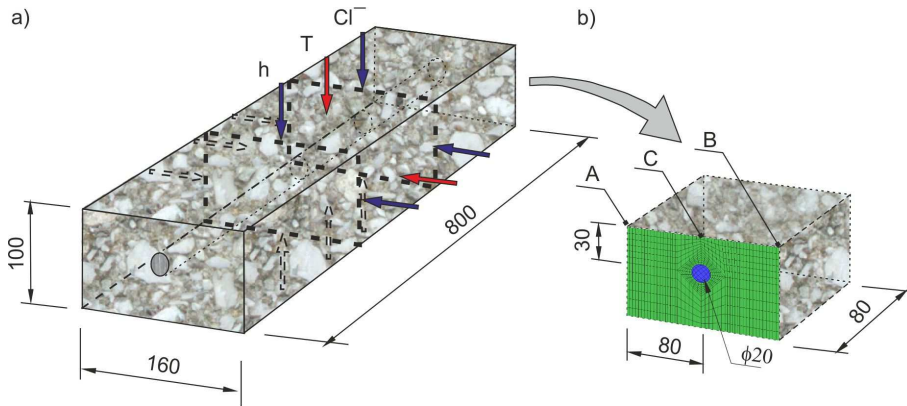


FIG. 4. The reinforced concrete element exposed to the environment and the impact of reinforcement corrosion: a) analysed element, b) numerical FEM model analysed in the paper.

The reinforced concrete element was assumed to be exposed to chloride ions (of the defined concentration  $\bar{C}_{Cl^-}$ ) and the effects of temperature  $\bar{T}$  and relative humidity  $\bar{h}$  variable over time, which are interval values (functions (22) and (23) simplified and based on the paper [3]).

$$\bar{h} = \bar{h}_{avg} - 0.5 (\bar{h}_{min} - \bar{h}_{max}) \sin(2\pi t), \quad \bar{h}_{avg} = 0.5 (\bar{h}_{min} + \bar{h}_{max}), \tag{22}$$

$$\bar{T} = \bar{T}_{avg} + 0.5 (\bar{T}_{min} - \bar{T}_{max}) \sin(2\pi t), \quad \bar{T}_{avg} = 0.5 (\bar{T}_{min} + \bar{T}_{max}), \tag{23}$$

where  $\bar{T}_{\max}$ ,  $\bar{T}_{\min}$  are interval variables defining the maximum and minimum values of the air temperature within a year,  $\bar{h}_{\max}$  and  $\bar{h}_{\min}$  are interval variables defining the maximum and minimum values of relative humidity within a year. The interval functions of the density of corrosion current  $\bar{i}$  and electrical resistance of concrete  $\bar{R}$  were determined using the modified empirical functions ( $\bar{i} = \bar{i}(t_s)$  for  $t \leq 14$  days,  $t_s = 14$  days) [3, 16, 17]:

$$\bar{i} = 0.9259 \left( 8.37 + 0.618 \ln \left( 1.69 \bar{C}_{mc} - 3034 \bar{T}^{-1} - 105^{-6} \bar{R} + 2.25 t^{-0.215} \right) \right), \quad (24)$$

$$\bar{R} = 90.537 \bar{h}^{-7.2548} \left[ 1 + \exp(5 - 50(1 - \bar{h})) \right], \quad (25)$$

where  $t$  is the exposure time in years, and the remaining values are interval values:  $\bar{i}$  is corrosion current density  $\mu\text{A}/\text{cm}^2$ ,  $\bar{C}_{mc}$  is chloride concentration on the reinforcement surface  $\text{kg}/\text{m}^3$  ( $\bar{C}_{mc} = \bar{m}_{cem} \bar{C}_{Cl^-}$ ),  $\bar{m}_{cem}$  is the cement content in the concrete  $\text{kg}/\text{m}^3$ ,  $\bar{C}_{Cl^-}$  is the concentration of chloride ions on the reinforcement surface  $\%_{cem}$ ,  $\bar{T}$  is the temperature at the reinforcement surface  $K$ ,  $\bar{R}$  is the electrical resistance of concrete  $\Omega$ , and  $\bar{h}$  is relative humidity 1.

Due to the lack of experimental data, extreme parameters of the numerical range  $\bar{X} = \langle X^-, X^+ \rangle$ , cf. Eqs (2) and (3), were determined from the following relationship:

$$X^- = X_0 - \Delta X_0, \quad X^+ = X_0 + \Delta X_0, \quad \Delta X_0 = 0.5\eta X_0, \quad (26)$$

where  $X_0$  is the mean value,  $\Delta X$  is the deviation from the mean value, and  $\eta$  is percentage deviation (this paper presents analyses made for minor deviations of 5% and 10%). In the case of parameters describing the function of temperature at the reinforcement surface and relative humidity, a range of numerical intervals specifying affine numbers  $T_{\max}$ ,  $T_{\min}$ ,  $h_{\max}$ ,  $h_{\min}$  was calculated using the formula (26), as for other variables; however, the deviation  $\Delta X_0$  was determined as a percentage of the mean value  $T_{\text{avg}}$  and  $h_{\text{avg}}$ , see, e.g., (22), (23). The results obtained were verified with the MC method [19]. Calculations using the MC method were made for 500 samples. The effects of chloride ions, temperature and relative humidity were analysed every hour over five years. Mean values, deviations from the mean value, infima  $X^- = \inf(X)$  and suprema  $X^+ = \sup(X)$  of parameters used in the calculations are compared in Table 1.

Changes in infima and suprema of interval functions, which restrained the infimum and supremum of temperature at the element surface  $\inf(T)$  and  $\sup(T)$  respectively, and of relative humidity  $\inf(h)$  and  $\sup(h)$  using the affine approach, are illustrated in Fig. 5. They refer to uncertainties  $\eta = 5\%$  and  $10\%$  and are marked with numbers 1 and 2 for the temperature, and numbers 4 and 5 for

TABLE 1. Comparison of average values, percentage deviations of environmental parameters and intervals describing the environmental data  $\bar{T}_{\max}$ ,  $\bar{T}_{\min}$ ,  $\bar{h}_{\max}$ ,  $\bar{h}_{\min}$  and chloride content in reinforced concrete element  $\bar{C}_{Cl-}$ .

Parameter	$X_0$	$X_{\text{avg}}$	$\Delta X_{5\%}$	$\Delta X_{10\%}$	$\bar{X}_{5\%}$	$\bar{X}_{10\%}$
Temperature, $\bar{T}_{\max}$ [°C]	25	15	0.375	0.75	[24.63, 25.38]	[24.25, 25.75]
Temperature, $\bar{T}_{\min}$ [°C]	5	15	0.375	0.75	[14.63, 15.38]	[14.25, 15.75]
Humidity, $\bar{h}_{\max}$ [1]	0.9	0.75	0.01875	0.0375	[0.88, 0.92]	[0.86, 0.94]
Humidity, $\bar{h}_{\min}$ [1]	0.6	0.75	0.01875	0.0375	[0.58, 0.62]	[0.56, 0.64]
Chloride content, $\bar{C}_{Cl-}$ [% of c.m.]	0.4	-	0.02	0.04	[0.39, 0.41]	[0.38, 0.42]
Cement mass, $\bar{m}_{cem}$ [kg/m <sup>3</sup> ]	350	-	17.5	35	[341.25, 358.75]	[332.5, 367.5]

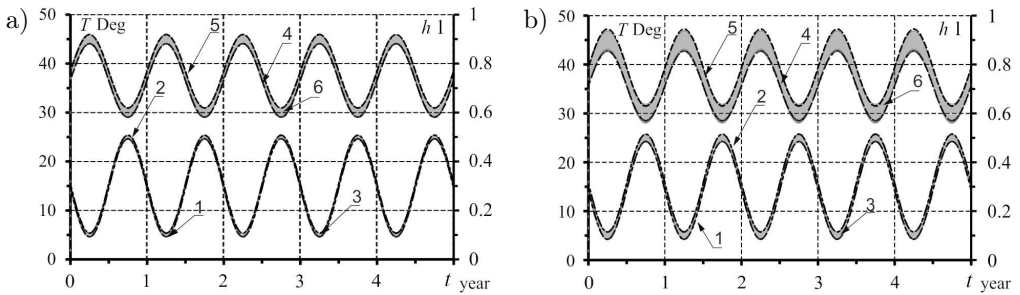


FIG. 5. Changes in the function of temperature  $T$  at the rebar surface and relative humidity  $h$  calculated on the basis of the affine approach and the MC method: a) 5% uncertainty of the model parameters, b) 10% uncertainty of the model parameters (description in the text).

relative humidity. The changes in temperature and relative humidity determined by the MC method are marked with numbers 3 and 6, respectively. The functions defining changes in infima and suprema of the function of corrosion current density  $\text{inf}(i)$  and  $\text{sup}(i)$ , marked with numbers 1 and 2, and electrical resistance of concrete  $\text{inf}(R)$  and  $\text{sup}(R)$  marked with numbers 4 and 5 respectively, for uncertainties analysed in the paper are illustrated in Fig. 6. The results obtained

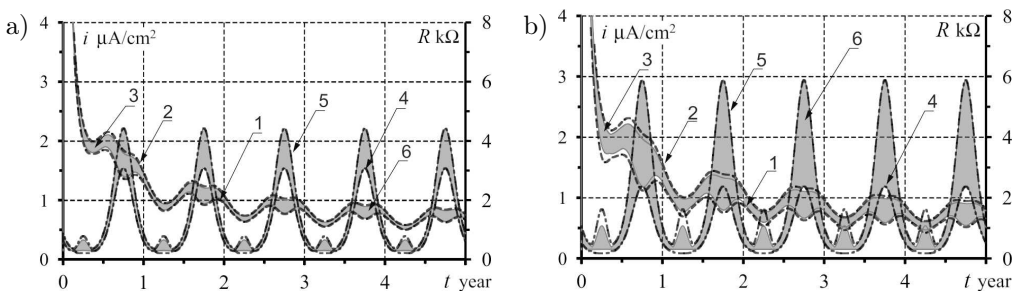


FIG. 6. Changes in the function of corrosion current density  $i$  and electrical resistance of concrete  $R$  calculated on the basis of the affine approach and the MC method: a) 5% uncertainty of the model parameters, b) 10% uncertainty of the model parameters (description in the text).

with the MC simulation for the corrosion current density and electrical resistance of concrete were marked with numbers 3 and 6, respectively.

For calculations, the mixture of  $\text{Fe}(\text{OH})_2$  and  $\text{Fe}(\text{OH})_3$  hydroxides was treated as corrosion products formed on the reinforcement surface. Parameters  $\alpha$  and  $\vartheta$  hydroxides (12) were based on the paper [25]: for iron (III) hydroxide,  $\alpha_{\text{Fe}(\text{OH})_3} = 0.523$ ,  $\vartheta_{\text{Fe}(\text{OH})_3} = 2.09$ , and iron (II) hydroxide,  $\alpha_{\text{Fe}(\text{OH})_2} = 0.622$ ,  $\vartheta_{\text{Fe}(\text{OH})_2} = 2.24$ . The density of iron ions equal to  $\rho_{\text{Fe}^{2+}} = 7850 \text{ kg/m}^3$  was used in calculations.

Parameters describing the chemical composition of corrosion products  $\bar{\alpha}$  and  $\bar{\vartheta}$ , defining porosity  $\bar{\gamma}_{wp}$ , and the width of the transition layer  $\bar{w}_{wp}$  (10)–(13), as well as the electrochemical equivalent of iron  $\bar{k}$  (reinforcing steel rebar – composition of iron and other admixtures), were considered as uncertain parameters (Table 2).

TABLE 2. Comparison of average values and percentage deviations of material parameters.

Parameter	$X_0$	$\Delta X_{5\%}$	$\Delta X_{10\%}$	$\bar{X}_{5\%}$	$\bar{X}_{10\%}$
Parameter, $\bar{\alpha} \cdot 10^2$ [1]	57.25	1.43	2.8625	[55.82, 58.68]	[54.39, 60.11]
Parameter, $\bar{\vartheta} \cdot 10^2$ [1]	216.5	5.41	10.825	[211.09, 221.91]	[205.68, 227.33]
The porosity of transition zone, $\bar{\gamma} \cdot 10^2$ [1]	55	1.38	2.75	[53.63, 56.38]	[52.25, 57.75]
The width of transition zone, $\bar{w}_{ws} \cdot 10^4$ [cm]	75	1.88	3.75	[73.13, 76.88]	[71.25, 78.75]
The electrochemical equivalent of iron, $\bar{k} \cdot 10^4$ [g/ $\mu\text{A}$ year]	91.2	2.28	4.56	[88.92, 93.48]	[86.64, 95.76]

The computer analysis of cracking and deformation of the concrete specimen was performed using the ATENA software. The Rankine model for elastic-plastic material with damage was used in the area under tension, whereas in other cases it was the Menetrey–Willam model (the material model was defined in the software as CC3DNonLinCementitious2). The following material parameters were used in calculations for concrete: Young’s modulus  $E_c = 38.5 \text{ GPa}$ , Poisson’s ratio  $\nu_c = 0.2$ , average compressive strength of concrete  $f_{cm} = 57.2 \text{ MPa}$ , average tensile strength of concrete  $f_{ctm} = 4 \text{ MPa}$ , and cracking energy  $G_f = 0.151 \text{ kN/m}$ . Steel reinforcement was specified as elastic and plastic material with hardening: Young’s modulus  $E_s = 200 \text{ GPa}$ , Poisson’s ratio  $\nu_s = 0.3$ , yield strength of steel  $f_y = 550 \text{ MPa}$ , and hardening modulus  $E_T = 10^4 \text{ MPa}$ . The interface material was characterised by the parameters: normal stiffness  $k_{nn} = 2 \cdot 10^8 \text{ MN/m}^3$ , tangential stiffness  $k_{tt} = 2 \cdot 10^8 \text{ MN/m}^3$ , cohesion coefficient  $c = 3 \text{ MPa}$ , friction coefficient  $\phi = 0.1$ , and tension strength  $f_t = 1 \text{ MPa}$ . In the analysis, the role of the interface layer was to stabilise the calculations.

The calculations performed were based on relationship (15) and provided the record of changes in the equivalent volume  $\bar{V}_{ekw}$  and effective volume  $\bar{V}_{eff}$  of corrosion products that have impact on the concrete cover. The results from calculations using the affine approach were compared with the results obtained from the MC method. The results of the above-mentioned analysis for the distribution of equivalent volumes  $\bar{V}_{ekw}$  are shown in Figs 7a and 7b respectively for the 5% and 10% uncertainty of the results and in Fig. 8 for distribution of the effective volume  $\bar{V}_{eff}$  for the same level of uncertainty. Numbers 1 and 2 in Figs 7 and 8 were assigned to changes in infima  $\inf(\bar{i})$  and suprema  $\sup(\bar{i})$  of corrosion current density determined in accordance with the affine approach, and number 3 denoted the distribution of corrosion current density  $i$  calculated using the MC method as in Fig. 6. Numbers 4 and 5 were assigned to the infimum  $\inf(\bar{V}_{ekw})$  and supremum  $\sup(\bar{V}_{ekw})$  of equivalent volume, and the infimum  $\inf(\bar{V}_{eff})$  and supremum  $\sup(\bar{V}_{eff})$  of the effective volume of corrosion products as shown in Fig. 8. The distribution of the equivalent and effective volume, whose values were determined using the MC method, are marked with number 6 in both figures.

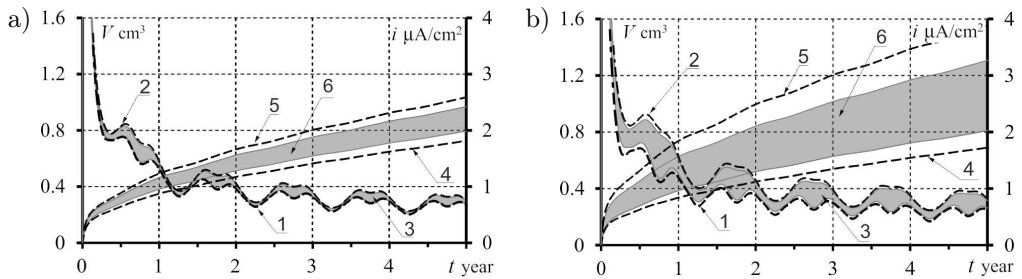


FIG. 7. Changes in the function of equivalent volume of corrosion products  $V_{ekw}$  depending on the corrosion current density  $i$  and time calculated on the basis of the affine approach and the MC method: a) 5% uncertainty of the model parameters, b) 10% uncertainty of the model parameters (description in the text).

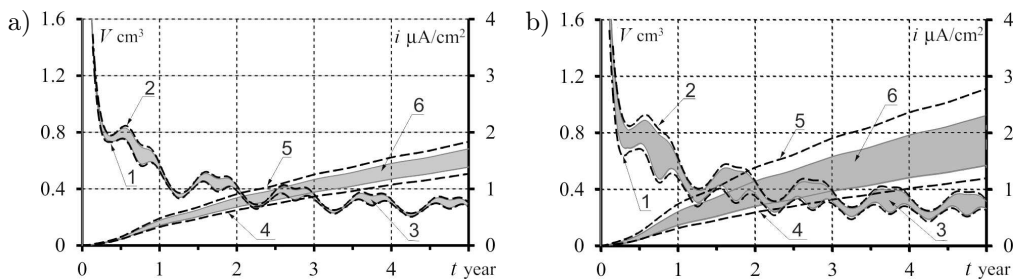


FIG. 8. Changes in the function of equivalent volume of corrosion products  $V_{eff}$  depending on the corrosion current density  $i$  and time calculated on the basis of the affine approach and the MC method: a) 5% uncertainty of the model parameters, b) 10% uncertainty of the model parameters (description in the text).

The results of the calculation of the extension of AB element edge,  $\Delta L_{AB}$ , and the width of cracks  $w_{cr}$  at point C in the reinforced concrete element were analysed in the next stage. To evaluate the width of the cracks and displacement field in the reinforced concrete element, the specimen was deemed to be exposed to volumetric strains caused by corrosion products accumulated on the rebar surface.

Strains defined by relationships (19)–(21) were applied to the rebar in a way similar to thermal loads specified in the theory of thermal stresses, in order to map the state of strains caused by deposition of corrosion products on the rebar side surface. The total increment of strain caused by deposition of corrosion products on the rebar side surface was divided into ten parts. To simplify calculations, increments of strains in the plane perpendicular to the rebar axis were used as loading during the total duration of corrosion. The loading was equivalent to the increments in volumetric strains for infimum  $\inf(\Delta\bar{\varepsilon}^V)$  and supremum  $\sup(\Delta\bar{\varepsilon}^V)$  bounds of the coordinates of increments of volumetric strain tensors. The graphical images showing the evolution of increments for corrosion volume strain tensor over time using affine numbers, bounds  $\inf(\Delta\bar{\varepsilon}^V)$  and  $\sup(\Delta\bar{\varepsilon}^V)$  in the plane perpendicular to the bar axis and the respective set of solutions obtained by using the MC method, are shown in Figs 9a and 9b respectively for 5% and 10% deviations. As in Fig. 6, numbers 1, 2, 3 in Fig. 9 designated the values of corrosion current density determined by the affine approach and the MC method. The values of suprema and infima for increments of volumetric strain coordinators determined using the affine approach  $\inf(\Delta\bar{\varepsilon}^V)$  and  $\sup(\Delta\bar{\varepsilon}^V)$  were designated with numbers 4 and 5, and the distribution of increments  $\Delta\bar{\varepsilon}^V$  determined by the MC method was designated with number 6.

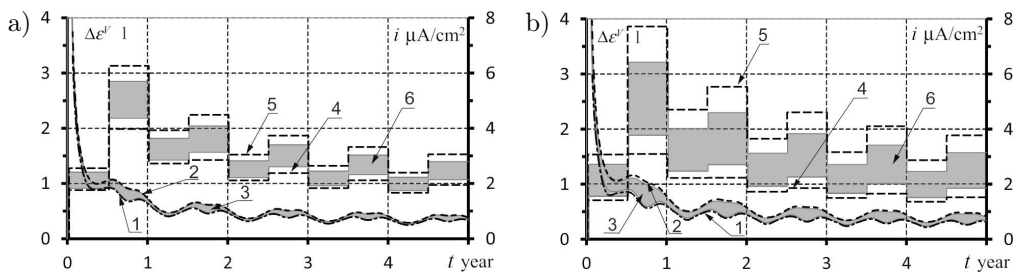


FIG. 9. Changes in the function of increments of volumetric strain  $\inf(\Delta\bar{\varepsilon}^V)$  and  $\sup(\Delta\bar{\varepsilon}^V)$  caused by an increment in corrosion products dependent on the corrosion current density  $i$  and time calculated on the basis of the affine approach and the MC method: a) 5% uncertainty of the model parameters, b) 10% uncertainty of the model parameters (description in the text).

The mechanical process of corrosion product degradation was simulated by considering equivalent increments of volumetric strain by analogy to the ana-

lysis of thermal stresses. The effect of corrosion products on the cover concrete was taken into account by exerting volumetric strains in the plane perpendicular to the rebar axis in accordance with the loading scheme shown in Fig. 9. Calculations were made which gave boundary (maximum and minimum) curves restraining a set of solutions for the crack width  $\min(w_{cr})$  and  $\max(w_{cr})$  of the element adjacent to the point  $C$  and extension of the edge  $AB$ ,  $\min(\Delta L_{AB})$  and  $\max(\Delta L_{AB})$  in the reinforced concrete element (Fig. 4). For that particular case, these calculations could be associated with the mean width of cracks in the element along the  $AB$  edge. Boundary envelopes of the extension of the element edge obtained on the basis of the assumption of 5% and 10% uncertainty of material parameters  $\min(\Delta L_{AB})$  and  $\max(\Delta L_{AB})$  are designated by numbers 1 and 2 in Figs 10a and 10b. The obtained effects including volumetric strains determined by the MC method  $\min(\Delta L_{AB})$  and  $\max(\Delta L_{AB})$  are designated by numbers 3 and 4. Crack widths  $w_{cr}$  in the finite element located near point  $C$  in the function of time and corrosion current density are illustrated in Figs 11a and 11b respectively for the uncertainties  $\eta = 5\%$  and  $10\%$ . Bound-

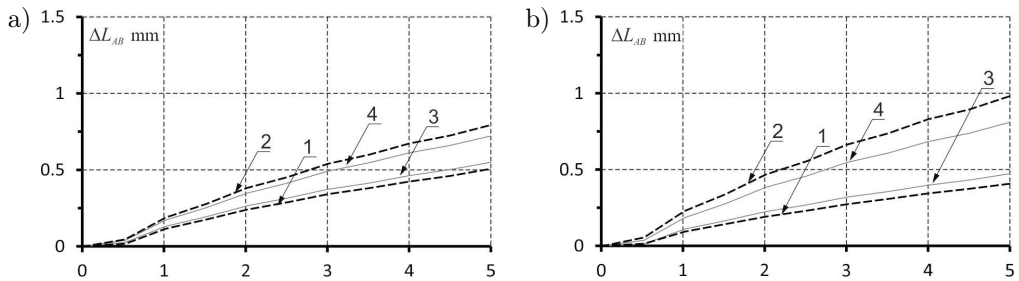


FIG. 10. Changes in minimum and maximum length of the element edge  $\Delta L_{AB}$  in the function of time for boundary increments of volumetric strains  $\inf(\Delta \varepsilon^V)$  and  $\sup(\Delta \varepsilon^V)$  determined on the basis of the affine approach and the MC method assuming the parameter uncertainty of a) 5%, b) 10% (description in the text).

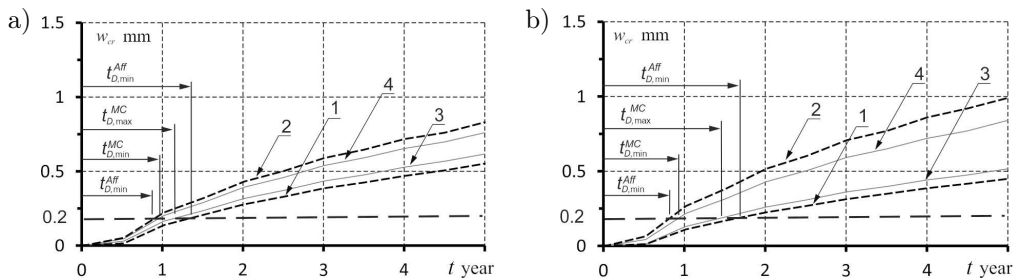


FIG. 11. Changes in minimum and maximum width of cracks  $w_{cr}$  in the finite element adjacent to point  $C$  as a function of time for boundary increments of volumetric strains  $\inf(\Delta \varepsilon^V)$  and  $\sup(\Delta \varepsilon^V)$  determined on the basis of the affine approach and the MC method assuming the parameter uncertainty of a) 5%, b) 10% (description in the text).

any values of crack width for volumetric strain increments determined by the affine approach were designated by numbers 3 and 4 respectively for  $\min(w_{cr})$  and  $\max(w_{cr})$ . Boundary values of crack width determined by the MC method were designated by numbers 1 and 2 respectively for  $\min(w_{cr})$  and  $\max(w_{cr})$ . Figure 11 also illustrates values for degradation time  $t_D$ , after which damage to concrete cover was observed. Degradation times were determined for the criterion of crack width  $w_{cr} = 0.2$  mm. Boundary times for the cover degradation by other criteria of crack width, determined for boundary increments of volumetric strain in accordance with the affine approach and the MC method, are compared in Table 3.

TABLE 3. Degradation times for reinforced concrete cover depending on the adopted method of calculations (the affine approach of the MC method), the criterion of allowable cracks  $w_{dop}^{\lim}$  and relative errors for time calculations.

Allowable crack [mm]	Deviation (uncertainty*) [%]	Time of degradation [month]				Relative error [%]	
		$t_{D,in}^{MC}$	$t_{D,max}^{MC}$	$t_{D,min}^{Aff}$	$t_{D,max}^{Aff}$	$\delta_{t,\alpha} = \frac{ t_{D,\alpha}^{MC} - t_{D,\alpha}^{Aff} }{t_{D,\alpha}^{MC}} \cdot 100$	
$w_{dop}^{\lim}$	$\eta$					$\delta_{t,\min}$	$\delta_{t,\max}$
0.1	5	8.25	9.5	8	10	3	5
0.2	5	12	15.5	11.5	18	4	16
0.3	5	19	23	17	27	11	17
0.4	5	25	33	22.5	38.5	10	17
0.5	5	33	45	30	53	9	18
0.1	10	8	12	7	10.5	13	13
0.2	10	12	19	10	22	17	16
0.3	10	17	29	14	35	18	21
0.4	10	22.5	42.5	19	51	16	20
0.5	10	30	57.5	23.5	69	20	20

\* Uncertainty percentage (5% or 10%) for material parameters.

Maps of damage and crack width in the analysed element at the end of the calculation procedure, after time  $t = 5$  years, are shown in Figs 12a–d. Maps presented in Figs 12a and 12b refer to the situation in which increments of strain tensors components  $\Delta\bar{\varepsilon}^V$  were determined at  $\eta = 5\%$  uncertainty of the material parameters  $\inf(\Delta\bar{\varepsilon}^V)$  and  $\sup(\Delta\bar{\varepsilon}^V)$ , respectively. Maps of damage shown in Figs 12c and 12d refer to the uncertainty of material parameters  $\eta = 10\%$ , respectively for  $\inf(\Delta\bar{\varepsilon}^V)$  and  $\sup(\Delta\bar{\varepsilon}^V)$ . Increments of strain tensors were calculated in accordance with the affine approach, cf. Fig. 9.

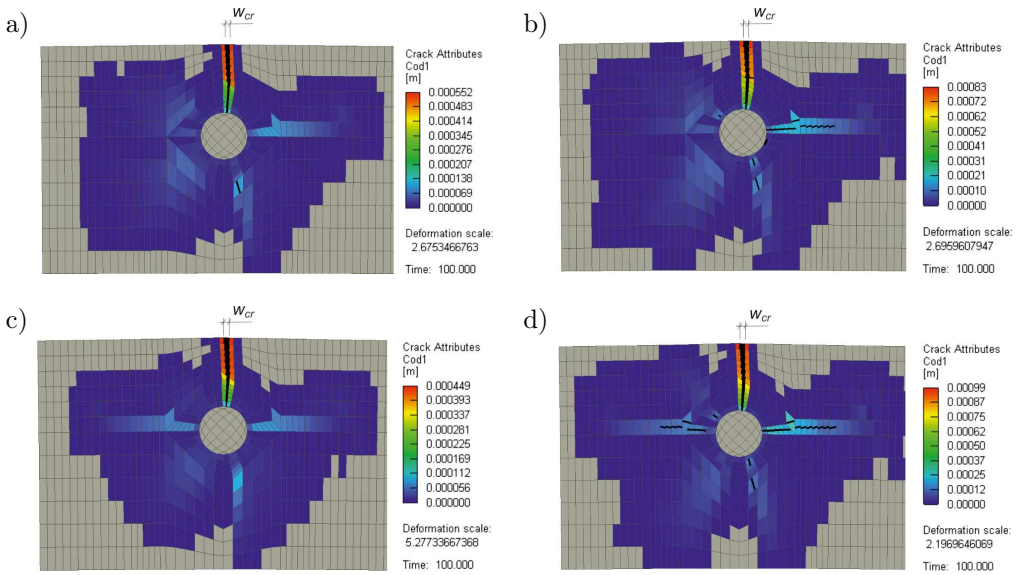


FIG. 12. The graphical images of a cracked concrete specimen at time  $t = 5$  years (step no. = 100) resulting from the impact of corrosion volumetric strains  $\Delta\bar{\varepsilon}^V$  (affine formulation) for the different uncertainties of material parameters  $\eta$ : a)  $\eta = 5\%$ ,  $\inf(\Delta\bar{\varepsilon}^V)$ , b) uncertainty  $\eta = 5\%$ ,  $\sup(\Delta\bar{\varepsilon}^V)$ , c)  $\eta = 10\%$ ,  $\inf(\Delta\bar{\varepsilon}^V)$ , d) uncertainty  $\eta = 10\%$ ,  $\sup(\Delta\bar{\varepsilon}^V)$ .

## 5. CONCLUSIONS

The modern approach to the design process of reinforced concrete structures assumes the crucial role of not only the safety issues, the durability and economic aspects, but also the investment impact on the environment and the society. The specified time of the service life  $t_{exp}$  of the designed structure understood as the sum of initiation times  $t_{in}$  and the degradation time  $t_D$  of the element cover caused by reinforcement corrosion is very important in the approach described in [33] on the hierarchical life-cycle design approach for designing reinforced concrete structures. The assessment of the durability of such structures can be troublesome due to the uncertainty of parameters used in the calculations and their effect on the service life, initiation and degradation of the structure (Fig. 1).

The algorithm developed in this paper uses affine numbers to assess the effect of reinforcement corrosion processes on the evolution of damage to the cover of reinforced concrete elements, taking into account minor uncertainties of material parameters. The obtained infima and suprema of equivalent volume  $\inf(\bar{V}_{ekw})$  and  $\sup(\bar{V}_{ekw})$  and effective volume  $\inf(\bar{V}_{eff})$  and  $\sup(\bar{V}_{eff})$ , and infima  $\inf(\Delta\bar{\varepsilon}^V)$  and suprema  $\sup(\Delta\bar{\varepsilon}^V)$  of coordinates of the tensor for volumetric strain increments of the plane perpendicular to the rebar axis, calculated taking into account the affine approach and the MC method, are close and the results do

not show a tendency for excessive overestimation of the solution (the number of calculation steps  $n_{cs} = 43\,800$ , frequency  $\Delta t = 1$  h, total time  $t = 5$  years).

The analysis of the results for uncertainty  $\eta = 5\%$  indicates a satisfactory correlation of the calculated results with those determined by the MC method. The relative error  $\delta_t$  of degradation time  $t_D$  for the boundary widths of cracks  $w_{cr}^{\text{lim}}$  for a 5-year process and time step  $\Delta t = 1$  h was within the range of 3–18% for boundary widths  $w_{cr}^{\text{lim}}$ , i.e., within the range of 0.1–0.5 mm. For greater uncertainties of  $\eta = 10\%$ , the relative error in estimating the degradation time of the cover for the boundary width  $w_{cr}^{\text{lim}}$  within the range of 0.1–0.5 mm, changed in the interval between 13% and 20%, which should be regarded as the satisfactory approximation of the final solution.

According to the author, the proposed approach provides a satisfactory description of the behaviour of structures over time. This approach can also be used to determine time intervals in which a cover can be damaged, the so-called degradation time –  $t_D$  of the structure (after taking into account problems related to mass transport, moisture and heat, problems on structure, the behaviour throughout its service life ( $t_{\text{exp}}$ ) can be described). A key element of this approach is also an intuitive method of describing the behaviour of model variables and obtained solutions such as numerical intervals  $\bar{x} = [x^-, x^+]$ . As probabilistic evaluation has limited possibilities for this type of issues, model parameters can be intuitively (based on expert evaluations) defined.

## REFERENCES

1. U. Angst, B. Elsener, C.K. Larsen, Ø. Vennesland, Critical chloride content in reinforced concrete – A review, *Cement and Concrete Research*, **39**(12): 1122–1138, 2009, doi: 10.1016/j.cemconres.2009.08.006.
2. U.M. Angst, Predicting the time to corrosion initiation in reinforced concrete structures exposed to chlorides, *Cement and Concrete Research*, **115**: 559–567, 2019, doi: 10.1016/j.cemconres.2018.08.007.
3. I. Balafas, C.J. Burgoyne, Environmental effects on cover cracking due to corrosion, *Cement and Concrete Research*, **40**(9): 1429–1440, 2010, doi: 10.1016/j.cemconres.2010.05.003.
4. A. Bentur, M.G. Alexander, A review of the work of the RILEM TC 159-ETC: Engineering of the interfacial transition zone in cementitious composites, *Materials and Structures*, **33**: 82–87, 2000, doi: 10.1007/BF02484160.
5. G. Bilotta, Self-verified extension of affine arithmetic to arbitrary order, *Le Matematiche*, **63**: 15–30, 2008.
6. A. Bossio, S. Imperatore, M. Kioumarsis, Ultimate flexural capacity of reinforced concrete elements damaged by corrosion, *Buildings*, **9**(7), 160, 2019, doi: 10.3390/buildings9070160.
7. H.G. Campos Silva, P. Garces Terradillos, E. Zornoza, J.M. Mendoza-Rangel, P. Castro-Borges, C.A. Juarez Alvarado, Improving sustainability through corrosion resistance of

- reinforced concrete by using a manufactured blended cement and fly ash, *Sustainability*, **10**(6), 2004, 2018, doi: 10.3390/su10062004.
8. S. Chen, H. Lian, X. Yang, Interval static displacement analysis for structures with interval parameters, *International Journal for Numerical Methods in Engineering*, **53**(2): 393–407, 2002, doi: 10.1002/nme.281.
  9. L.T.N. Dao, V.T.N. Dao, S.H. Kim, K.Y. Ann, Modeling steel corrosion in concrete structures – part 1: A new inverse relation between current density and potential for the cathodic reaction, *International Journal of Electrochemical Science*, **5**(3): 302–313, 2010.
  10. L.T.N. Dao, V.T.N. Dao, S.H. Kim, K.Y. Ann, Modeling steel corrosion in concrete structures – part 2: A unified adaptive finite element model for simulation of steel corrosion, *International Journal of Electrochemical Science*, **5**(3): 314–326, 2010.
  11. L.H. De Figueiredo, J. Stolfi, Affine arithmetic: concepts and applications, *Numerical Algorithms*, **37**(1–4): 147–158, 2004, doi: 10.1023/B:NUMA.0000049462.70970.b6.
  12. D. Degrauwe, G. Lombaert, G. De Roeck, Improving interval analysis in finite element calculations by means of affine arithmetic, *Computers and Structures*, **88**(3–4): 247–254, 2010, doi: 10.1016/j.compstruc.2009.11.003.
  13. H. El-Owny, *Hansen’s generalized interval arithmetic realized in C-XSC*, Bergische Universität Wuppertal, Wuppertal, Germany, pp. 1–52, 2006.
  14. S. Guzmán, J.C. Gálvez, J.M. Sancho, Cover cracking of reinforced concrete due to rebar corrosion induced by chloride penetration, *Cement and Concrete Research*, **41**(8): 893–902, 2011, doi.org/10.1016/j.cemconres.2011.04.008.
  15. P.O. Iqbal, T. Ishida, Modeling of chloride transport coupled with enhanced moisture conductivity in concrete exposed to marine environment, *Cement and Concrete Research*, **39**(4): 329–339, 2009, doi: 10.1016/j.cemconres.2009.01.001.
  16. Y. Liu, R.E. Weyers, Comparison of guarded and unguarded linear polarization CCD devices with weight loss measurements, *Cement and Concrete Research*, **33**(7): 1093–1101, 2003, doi: 10.1016/S0008-8846(03)00018-8.
  17. W. López, J.A. González, Influence of the degree of pore saturation on the resistivity of concrete and the corrosion rate of steel reinforcement, *Cement and Concrete Research*, **23**(2): 368–376, 1993, doi: 10.1016/0008-8846(93)90102-F.
  18. G. Manson, Calculating frequency response functions for uncertain systems using complex affine analysis, *Journal of Sound and Vibration*, **288**(3): 487–521, 2005, doi: 10.1016/j.jsv.2005.07.004.
  19. N. Metropolis, S. Ulam, The Monte Carlo method, *Journal of the American Statistical Association*, **44**(247): 335–341, 1949, doi: 10.2307/2280232.
  20. A. Michel, B.J. Pease, A. Peterová, M.R. Geiker, H. Stang, A.E.A. Thybo, Penetration of corrosion products and corrosion-induced cracking in reinforced cementitious materials: Experimental investigations and numerical simulations, *Cement and Concrete Composites*, **47**: 75–86, 2014, doi: 10.1016/j.cemconcomp.2013.04.011.
  21. R.E. Moore, Interval analysis, *Mathematics of Computation*, **22**(101): 219–222, 1968, doi: 10.2307/2004792.
  22. O. Na, Y. Xi, Parallel finite element model for multispecies transport in nonsaturated concrete structures, *Materials*, **12**(17), 2764, 2019, doi: 10.3390/ma12172764.

23. J. Ožbolt, F. Oršanić, G. Balabanić, Modeling influence of hysteretic moisture behavior on distribution of chlorides in concrete, *Cement and Concrete Composites*, **67**: 73–84, 2016, doi: 10.1016/j.cemconcomp.2016.01.004.
24. J. Ožbolt, F. Oršanić, G. Balabanić, Modelling processes related to corrosion of reinforcement in concrete: coupled 3D finite element model, *Structure and Infrastructure Engineering*, **13**(1): 135–146, 2017, doi: 10.1080/15732479.2016.1198400.
25. S.J. Pantazopoulou, K.D. Papoulia, Modeling cover-cracking due to reinforcement corrosion in RC structures, *Journal of Engineering Mechanics*, **127**(4): 342–351, 2001.
26. K.G. Papakonstantinou, M. Shinozuka, Probabilistic model for steel corrosion in reinforced concrete structures of large dimensions considering crack effects, *Engineering Structures*, **57**: 306–326, 2013, doi: 10.1016/j.engstruct.2013.06.038.
27. S.M. Rump, M. Kashiwagi, Implementation and improvements of affine arithmetic, *Nonlinear Theory and Its Applications*, IEICE, **2**(3): 1101–1119, 2015, doi: 10.1588/nolta.2.1101.
28. A. Saetta, R. Scotta, R. Vitaliani, Mechanical behavior of concrete under physical-chemical attacks, *Journal of Engineering Mechanics*, **124**(10): 1100–1109, 1998, doi: 10.1061/(ASCE)0733-9399(1998)124:10(1100).
29. J. Stolfi, L.H. de Figueiredo, Self-validated numerical methods and applications, *CiteSeerX*, 1–122, 1997.
30. C. Suwito, Y. Xi, The effect of chloride-induced steel corrosion on service life of reinforced concrete structures, *Structure and Infrastructure Engineering*, **4**(3): 177–192, 2008, doi: 10.1080/15732470600688699.
31. J. Szymenderski, W. Machczyński, K. Budnik, Modeling effects of stochastic stray currents from D.C. traction on corrosion hazard of buried pipelines, *Energies*, **12**(23), 4570, 2019, doi: 10.3390/en12234570.
32. K. Tuutti, *Corrosion of Steel in Concrete*, Swedish Cement and Concrete Research Institute, Stockholm, 1982.
33. Z. Wang, W. Jin, Y. Dong, D.M. Frangopol, Hierarchical life-cycle design of reinforced concrete structures incorporating durability, economic efficiency and green objectives, *Engineering Structures*, **157**: 119–131, 2018, doi: 10.1016/j.engstruct.2017.11.022.
34. B. Wieczorek, T. Krykowski, Application of damage mechanics rules to evaluate the growth of corrosive deformations in transition layer [in Polish: Zastosowanie reguł mechaniki uszkodzeń do oceny wzrostu odkształceń korozyjnych w warstwie przejściowej], *Ochrona przez korozją*, **60**(1): 5–8, 2017, doi: 10.15199/40.2017.1.1.
35. W. Zhu, K. Yu, Y. Xu, K. Zhang, X. Cai, A prediction model of the concrete cracking induced by the non-uniform corrosion of the steel reinforcement, *Materials*, **13**(4): 830, 2020, doi: 10.3390/ma13040830.
36. T. Krykowski, T. Jaśniok, F. Recha, M. Karolak, A cracking model for reinforced concrete cover, taking account of the accumulation of corrosion products in the ITZ layer, and including computational and experimental verification, *Materials*, **13**, 2020 [in print].

*Received June 10, 2020; revised version September 7, 2020.*